Chemical Engineering Journal 266 (2015) 133–140

Contents lists available at ScienceDirect

Chemical Engineering Journal

journal homepage: www.elsevier.com/locate/cej

Photocatalytic inactivation of bacterial spores using TiO_2 films with silver deposits

Silvia M. Zacarías [a,b], María L. Satuf [a], María C. Vaccari [b], Orlando M. Alfano [a,*]

[a] Instituto de Desarrollo Tecnológico para la Industria Química (Universidad Nacional del Litoral and Consejo Nacional de Investigaciones Científicas y Técnicas), Ruta Nacional N° 168, 3000 Santa Fe, Argentina
[b] Facultad de Bioquímica y Ciencias Biológicas, Universidad Nacional del Litoral, Ruta Nacional N° 168, Paraje el Pozo, 3000 Santa Fe, Argentina

HIGHLIGHTS

- Inactivation activity of undoped and silver doped TiO_2 catalysts was evaluated.
- *Bacillus subtilis* spores over TiO_2 films were irradiated with artificial UV-A light.
- Superior activity was found when the silver content of the coatings was increased.
- Maximum quantum efficiency was found with the sample containing 1.09 wt.% Ag/TiO_2.
- Lower efficiency was observed with an excess of dopant metal.

GRAPHICAL ABSTRACT

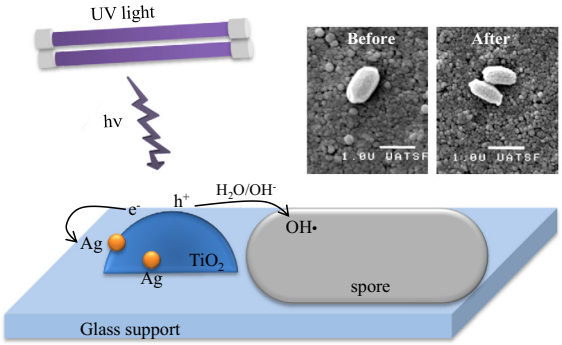

ARTICLE INFO

Article history:
Received 6 August 2014
Received in revised form 16 December 2014
Accepted 18 December 2014
Available online 25 December 2014

Keywords:
Titanium dioxide
Silver
Bacillus subtilis spores
Inactivation
Quantum efficiency

ABSTRACT

The present work evaluates the enhancement of the photocatalytic inactivation of bacterial spores employing TiO_2 films with silver deposits compared to TiO_2 films without metal deposition. *Bacillus subtilis* spores spread over TiO_2 films with different silver contents were irradiated with artificial UV-A light. The performances of the coatings were evaluated by the quantum efficiency parameter, which relates the inactivation rate with the radiation absorption rate by the coating. Spectral diffuse transmittance and reflectance measurements of the films were carried out to evaluate the fraction of energy absorbed by the coatings. TiO_2 and Ag/TiO_2 films characterization also included X-ray Diffraction (XRD), Atomic Force Microscopy (AFM), X-ray photoelectron spectroscopy (XPS), and Scanning Electron Microscopy (SEM). A notable increase in the photocatalytic inactivation was observed by increasing the silver content of the coatings, reaching a maximum quantum efficiency with the sample containing 1.09 wt.% Ag/TiO_2. The addition of higher amounts of silver rendered lower inactivation, thus indicating the existence of an optimum Ag/TiO_2 relation.

1. Introduction

Pollution of indoor air by pathogenic microorganisms represents a major problem in modern societies, where people spend most of their time indoors [1]. Bioaerosols, containing viruses, bacteria, and fungi, can be responsible for infectious diseases, toxic reactions, and allergic responses. Consequently, research on disinfection technologies to control bioaerosols in air constitutes an area of great scientific interest [2,3].

Photocatalysis with TiO_2 has many advantages over conventional technologies to remove microorganisms from air. Mainly,

* Corresponding author. Tel.: +54 342 4511546; fax: +54 342 4511170.
E-mail address: alfano@santafe-conicet.gov.ar (O.M. Alfano).

http://dx.doi.org/10.1016/j.cej.2014.12.074
1385-8947/

Nomenclature

ATCC	American Type Culture Collection
CFU	Colony Forming Units
$e_f^{a,s}$	surface rate of photon absorption by the TiO_2 catalytic films (photon cm^{-2} h^{-1})
k	apparent kinetic constant (h^{-1})
N	viable spore concentration (CFU cm^{-2})
N_0	initial viable spore concentration (CFU cm^{-2})
$q_{f,in}$	local radiative flux that reaches the TiO_2 catalytic films (photon cm^{-2} h^{-1})
$q_{f,tr}$	local radiative flux transmitted through the TiO_2 catalytic films (photon cm^{-2} h^{-1})
$q_{f,rf}$	local radiative flux reflected by the TiO_2 catalytic films (photon cm^{-2} h^{-1})
R	reflectance (dimensionless)
t	time (h)
T	transmittance (dimensionless)

Greek letters

α_f	fraction of energy absorbed by the TiO_2 films (dimensionless)
η_{abs}	quantum efficiency of inactivation (CFU $photon^{-1}$)
φ_λ	normalized fraction of the radiation that reaches the coated plates at wavelength λ (dimensionless)

Subscripts

λ	relative to a specific wavelength
A_{irr}	relative to the irradiated area
f	relative to a property of the TiO_2 film
fg	relative to a property of the TiO_2 film + glass
g	relative to a property of the bare borosilicate glass plate

Special symbol

$\langle\rangle$	average

it can effectively destroy biological species, unlike filtration or ventilation. Additionally, it does not produce any hazardous by-products, as is the case of chemical disinfection, and it can be operated under ambient conditions of temperature and pressure.

Numerous studies on the photocatalytic inactivation of different types of microorganisms in air have been reported in the literature and have been summarized in recent reviews [4–6]. However, studies on the inactivation of resistant forms of microorganisms, such as bacterial and fungal spores, are less frequent [7]. Specifically, spores of *Bacillus* species are much more resistant to adverse environmental conditions and inactivation technologies than vegetative cells and can therefore be employed as biological indicators to evaluate disinfection processes [8].

Due to the unique characteristics of the spore's structure, mainly the complexity and thickness of the cell envelope, TiO_2 inactivation of *Bacillus* endospores is relatively slow and considerable efforts are being made to enhance the process [9]. The approaches to increase the inactivation rate include the addition of metal and nonmetal dopants to the photocatalyst. Kozlova et al. [10] reported the photocatalytic mineralization of *Bacillus thuringiensis* (mix of vegetative cells with 20–30% of spores) over TiO_2 and Pt/TiO_2 under UVA irradiation. Microorganisms were loaded over photocatalytic films from aerosols. Pt/TiO_2 coated plates showed increased rate of mineralization. Particularly, the enhancement of the photocatalytic inactivation of bacteria with silver loaded TiO_2 has been demonstrated in liquid and gas phase [9,11–16]. Besides its well documented bactericidal effect, silver can act as electron acceptor, thus reducing the recombination of electrons and holes in the catalyst and improving its performance. Also, silver can generate hydroxyl radicals and contribute to the activity of TiO_2 [5]. In this context, the calculation of efficiency parameters constitutes a helpful tool for comparing different photocatalytic systems [17,18].

The present work evaluates the enhancement of the photocatalytic inactivation of bacterial spores employing TiO_2 films with silver deposits. *Bacillus subtilis* spores (model organism of biological contaminants present in air) spread over TiO_2 films with different silver contents were irradiated with artificial UV-A light. The performances of the coatings were evaluated by the quantum efficiency parameter. Specifically, the value of the quantum efficiency of inactivation, which relates the inactivation rate with the energy absorbed by the coating, shows how efficiently the absorbed radiation is employed to inactivate microorganisms, giving an indirect insight into the photocatalytic mechanism. Also, it can help to design better coatings, as the results can evidence deficient contact between bacteria and photocatalyst, or poor absorption of radiation.

Measurements of the spectral diffuse transmittance and reflectance of bare and catalyst-coated glass plates were obtained with a spectroradiometer equipped with an integrating-sphere reflectance attachment. Then, the net-radiation method was used to compute the fraction of energy effectively absorbed by the photocatalyst. Additional characterization to evaluate the effect of silver on the surface properties of the films included XRD, AFM, XPS and SEM.

2. Experimental materials and procedures

2.1. Materials

2.1.1. Bacterial strain and spore culture

B. subtilis (strain ATCC 6633) spores were used as the model microorganism. To obtain the spore suspension, the technique proposed by Shehata and Collins [19] was followed. The sporulation medium, consisting of nutrient agar (Merck Chemicals) with 0.05% $MgSO_4$ and 0.05% $MnSO_4$, was inoculated with 5 mL of *B. subtilis* on nutrient broth, and incubated at 30 °C for 10 days. Subsequently, spores were washed several times with sterile saline solution (0.9%) to remove vegetative cells. Finally, spores were suspended in sterile distilled water and stored at 4 °C.

2.1.2. Titanium dioxide

Titanium dioxide AEROXIDE®TiO_2 P 25 (Evonik, Germany) was employed for inactivation assays (BET specific surface area: 50 ± 15 m^2/g, TiO_2-content $\geqslant$ 99.5 wt.%, SiO_2-content $\leqslant$ 0.2 wt.%, tapped density 130 g/L).

2.2. Experimental setup

The photocatalytic reactor employed is sketched in Fig. 1 [18]. It consists of a radiation emitting system and an irradiation compartment with a support to hold the glass plates while spore samples are being irradiated.

The radiation emitting system contains seven black light lamps (Philips TL 4W/08 F4 T5/BLB) in horizontal parallel arrangement. The emission wavelength range of the lamps is comprised between 300 nm and 400 nm, with a maximum emission peak at 350 nm.

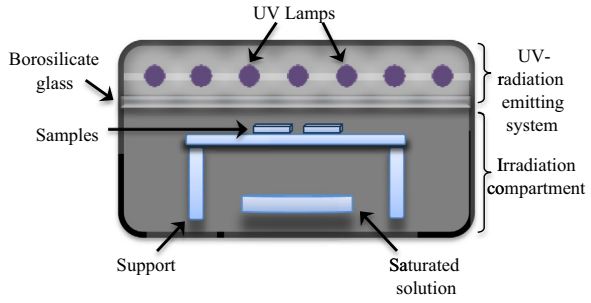

Fig. 1. Schematic representation of the experimental setup.

The irradiation compartment is a metallic rectangular box with a removable borosilicate glass plate. UV radiation generated by the emitting system enters the compartment through the glass cover, which also prevents contamination of spore samples during irradiation. Photocatalytic plates with the spore samples were placed horizontally on the sample holder, in the central zone of irradiation compartment, where the radiation flux was almost uniform [20]. This support, prior to each assay, was autoclaved at 121 °C for 15 min. To ensure an atmosphere of high relative humidity, a Petri dish containing ammonium sulfate saturated solution was included in the irradiation compartment. High relative humidity would enhance the production of hydroxyl radicals, thus improving the effectiveness of the inactivation process.

During all experimental runs, temperature and relative humidity inside the irradiation compartment, measured with a thermo-hygrometer (TH PTH8708 Mannix Pen), were kept constant at 40 °C and 70%, respectively. This compartment, prior to each inactivation test, was sterilized in an oven at 160 °C for 2 h.

2.3. Experimental procedure

2.3.1. Preparation of photocatalytic plates

Borosilicate glass plates of 2 cm × 2 cm were used as support to immobilize the catalyst. This material was chosen due to its high transmittance in the UV-A region and its resistance to the high temperatures required for the coating process. Before TiO_2 immobilization, the glass plates were cleaned-up with soap and water and then immersed in a solution containing 20 g of potassium hydroxide, 250 mL of isopropyl alcohol, and 250 mL of ultrapure water. The plates were kept in contact with the washing solution for 24 h. To remove any trace of organic material, the glass fragments were finally heated at 500 °C for 8 h.

2.3.2. TiO_2 coating

The "dip-coating" technique was employed to obtain the photocatalytic films over the glass plates. This method basically consisted of immersing the glass to be coated in a suspension containing the catalyst, and then withdrawing it at a controlled speed. The catalyst suspension was prepared by dispersing 150 g of TiO_2 in 1 L of ultrapure water (Osmoion Ultrapure Water, Apema). The pH was adjusted to 1.5 with HNO_3 [21]. The plates were withdrawn from the catalyst suspension at a speed of 3 cm min^{-1}, and then dried at 110 °C for 24 h. Finally, the coated plates were calcined at 500 °C for 2 h to increase the coating adhesion and to induce the anatase phase formation.

A second TiO_2 coating was obtained by repeating the procedure described above. According to a previous study [18], two coatings cycles rendered the best spore inactivation efficiencies.

The amount of TiO_2 deposited on the glass plates was measured by a spectrophotometric procedure adapted from Jackson et al. [22] that involves the digestion of the photocatalyst followed by a colorimetric detection [18].

2.3.3. Ag deposition

Different silver amounts were added to the coated plates by means of a photodeposition technique [12].The TiO_2 coated glasses were immersed in silver nitrate solutions (Merck, $AgNO_3$ in HNO_3, 0.5 M) of different concentrations and irradiated with UV-A lamps (actinic lamps BL Philips 20 W) for 2 h to reach the complete reduction of silver. 2-Propanol was added as sacrificial organic compound to scavenge hydroxyl radicals and holes. As a final step, the Ag/TiO_2 coated glasses were dried at 100 °C for 15 min.

Atomic Absorption Spectroscopy (AAS, Perkin Elmer AAnalyst 800) was employed to quantify the silver content of the coated plates. The analytical technique involved the following steps: First, Ag/TiO_2 coated plates were immersed in concentrated nitric acid and sonicated for 15 min. Subsequently, an aliquot of the nitric solution was filtered through a 0.4 μm filter, and finally the filtrate was analyzed by AAS. Measurements were performed in duplicate. Ag concentration is expressed in weight by weight percent (wt.%) and refers to the mass of Ag in relation to the mass of TiO_2 contained in each glass plate.

2.3.4. Surface rate of photon absorption

Photon absorption in the TiO_2 film is the initial step of the photocatalytic process. When modeling the radiation absorption of a thin layer of TiO_2 immobilized on the surface of an inert support, it is appropriate to refer the photon absorption rate per unit area of irradiated TiO_2-coated surface. As a result, the inactivation rate of microorganisms depends on the Surface Rate of Photon Absorption ($e_f^{a,s}$ or SRPA).

When a radiation beam traverses the TiO_2 film (Fig. 2), its intensity will change due to three events: (a) part of the energy will be absorbed by the film, (b) part of the energy will be transmitted through the film, and (c) part of the energy will be reflected by the film.

By applying a local radiative energy balance in terms of the local net radiation fluxes, the SRPA at each point of the photocatalytic film can be calculated as

$$e_f^{a,s}(x) = q_{f,in}(x) - q_{f,tr}(x) - q_{f,rf}(x) \quad (1)$$

where $q_{f,in}$ is the local radiative flux that reaches the coated plate, $q_{f,tr}$ the local radiative flux transmitted through catalytic film, and $q_{f,rf}$ the local radiative flux reflected by the TiO_2 surface. By performing the average of the local fluxes over the irradiated area, the average SRPA can be obtained as

$$\langle e_f^{a,s}\rangle_{A_{irr}} = \langle q_{f,in}\rangle_{A_{irr}} - \langle q_{f,tr}\rangle_{A_{irr}} - \langle q_{f,rf}\rangle_{A_{irr}} \quad (2)$$

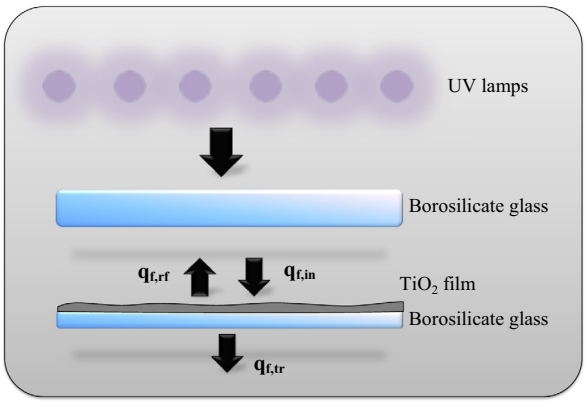

Fig. 2. Schematic representation of local radiative flux over the coated plate.

Eqs. (1) and (2) are valid for monochromatic and polychromatic radiation, as long as the same wavelength range is considered for every term. For monochromatic radiation, the SRPA can also be expressed as a function of the incident radiation flux as

$$\langle e_f^{a,s}\rangle_{A_{irr}} = \langle q_{f,in}\rangle_{A_{irr}} \alpha_{f,\lambda} \quad (3)$$

where $\alpha_{f,\lambda}$ is the fraction of energy absorbed by the TiO_2 film at wavelength λ. Similarly, for polychromatic radiation

$$\langle e_f^{a,s}\rangle_{A_{irr}} = \langle q_{f,in}\rangle_{A_{irr}} \sum_{\lambda} \alpha_{f,\lambda}\varphi_{\lambda} \quad (4)$$

where φ_{λ} is the normalized fraction of the radiation that reaches the coated plates at wavelength λ, and $\sum_{\lambda}$. the summation over the useful wavelength range. φ_{λ} takes into account the spectral emission of the lamps and the slight modification of the lamp spectrum produced by the absorption of the borosilicate glass that separates the lamps from the irradiation compartment, mainly at wavelengths lower than 325 nm. The spectral emission of the lamps and the transmittance of the borosilicate glass between 300 and 400 nm can be found in Ref. [18].

The average value of the incident radiation flux $\langle q_{f,in}\rangle_{A_{irr}}$, experimentally measured with a radiometer (IL 1700-SED005-WBS 320), was 1.21×10^{19} photon cm^{-2} h^{-1}. Measurements were carried out by placing the radiometer sensor facing the radiation emitting system at different positions on a plane located at 4.5 cm from the lamps. It should be noted that the measurement of the incident radiation flux was performed by placing the radiometer below the borosilicate glass that separates the lamps from the irradiation compartment; therefore, the value obtained takes into account the absorption of the aforementioned borosilicate glass. To ensure uniform irradiation conditions over the TiO_2 plates, only the central zone of the irradiation compartment was employed in the experiments, where the maximum difference between the most illuminated area and the less illuminated one was 17% [20].

The values of φ_{λ} for every wavelength were obtained from data of the spectral emission of the lamps given by the manufacturer.

The absorbed fraction of energy $\alpha_{f,\lambda}$ can be calculated as:

$$\alpha_{f,\lambda} = 1 - T_{f,\lambda} - R_{f,\lambda} \quad (5)$$

where $T_{f,\lambda}$ and $R_{f,\lambda}$ represent the fraction of energy transmitted and reflected by the TiO_2 film at wavelength λ. $T_{f,\lambda}$ and $R_{f,\lambda}$ cannot be directly measured, but they can be computed from the experimental values of diffuse transmittance (T) and reflectance (R) of the coated and bare plates. The following expressions, obtained by applying the Net-Radiation method [23] to the catalytic plate, relate the values of transmittance and reflectance of the TiO_2 film (f), the bare plate (glass, g), and the coated plate (film + glass, fg):

$$T_{fg,\lambda} = \frac{T_{f,\lambda}T_{g,\lambda}}{1 - R_{f,\lambda}R_{g,\lambda}} \quad (6)$$

$$R_{fg,\lambda} = R_{f,\lambda} + \frac{R_{g,\lambda}T_{f,\lambda}^2}{1 - R_{f,\lambda}R_{g,\lambda}} \quad (7)$$

By rearranging Eqs. (6) and (7), the values of $T_{f,\lambda}$ and $R_{f,\lambda}$ can be calculated. Diffuse transmittance and reflectance measurements of the coated and bare plates were carried out with a spectrophotometer Optronic OL series 750, equipped with a reflectance integrating sphere (OL 740-70). A detailed description of the methodology employed can be found elsewhere [18].

2.3.5. Additional characterization of the films

X-ray diffraction patterns were measured using Shimadzu XD-D1 X-ray diffractometer with monochromatic high intensity Cu Kα irradiation, 2θ range from 23° to 70° by 1° s^{-1} steps, operated at 30 kV and 40 mA. AFM measurements were performed in air using a commercial Nanotec Electronic System (Nanotec Electrónica S.L., Madrid, Spain) operating in tapping-mode at room temperature. Acquisition and image processing were performed using the WS×M free software [24]. XPS analysis was performed with a Specs Multitechnique instrument equipped with dual X-ray source Mg/Al and a hemispherical analyzer PHOIBOS 150 in the FAT mode. Spectra were obtained with a pass energy of 30 eV and Mg anode operated at 200 W. Pressure during measurements was smaller than 2×10^{-8} mbar. Surface images were obtained by means of a Scanning Electron Microscope (JEOL, JSM-35C) equipped with an acquisition system of digital images (SemAfore). The observation was made in the secondary electron images mode using an accelerating voltage of 22 kV.

2.4. Photocatalytic experiments

Inactivation of *B. subtilis* spores was evaluated over coatings with TiO_2 and TiO_2 with four different amounts of Ag deposited: 0.35, 0.47, 1.09 and 2.15 wt.%, expressed as the mass of Ag in relation to the mass of TiO_2 of the coated plate. The selection of the silver content of the films was based on previous studies [12,16].

Before starting every inactivation assay, a fraction of the spore suspension was maintained at 80 °C for 10 min (heat shock) to remove any remaining vegetative cell. Next, 10 μL aliquots of the spore suspension of approximately 5.0×10^7 CFU mL^{-1} were spread over the coated plates covering an area of 1.5 cm × 1.5 cm. The plates were maintained at 30 °C for 1 h to dry the samples. Then, the dry plates were placed in the irradiation compartment and exposed to UV-A radiation for different time periods (2, 4 and 6 h). After the programmed irradiation time for each sample, the photocatalytic plates were removed and the remaining viable spores counted. Irradiation assays were performed with dry bacterial spores to represent the environmental conditions in which spores are disseminated by air over dust particles.

To perform the counting of viable spores, each irradiated plate was placed in a tube with 10 mL of sterile extraction solution (0.1% peptone in distilled water). Then, the sample was gently scraped with a spatula to separate the spores from the surface of the plate. Subsequently, the tube with the plate, the spatula and the extraction solution were stirred at 200 rpm for 15 min. Finally, aliquots of 1 mL of the resulting suspension were spread onto nutrient agar plates (Merck Chemicals), incubated at 30 °C for 48 h, and the colony forming units (CFU) counted. The tests were repeated twice for each experimental condition studied, and the counting of the viable spores of each repetition was made in duplicate.

The decay of viable spores as a function of the irradiation time was fitted with the exponential equation:

$$N = N_0 \exp(-kt) \quad (8)$$

where N (CFU cm^{-2}) is the bacterial concentration at time t, N_0 (CFU cm^{-2}) the initial bacterial concentration, k (h^{-1}) an apparent kinetic constant, and t (h) the irradiation time.

The performance of the coatings was objectively assessed by calculation of the quantum efficiency of inactivation η_{abs} (or absolute efficiency), defined as the ratio of the initial rate of inactivation $-(dN/dt)|_{t=0}$ to the radiation energy absorbed by the coated film, within the range of useful wavelengths [18]:

$$\eta_{abs} = \frac{-(dN/dt)|_{t=0}}{\langle e_f^{a,s}\rangle_{A_{irr}}} \quad (9)$$

The initial rates of inactivation of the different assays were obtained by calculating the first derivative of the corresponding fitting curves (Eq. (8)) at $t = 0$.

3. Results and discussion

3.1. Characterization of the photocatalytic films

Fig. 3 presents the diffuse transmittance and reflectance spectra of the glass plates coated with TiO_2 without Ag and with different amounts of Ag. Significant differences in the transmittance spectra at wavelengths longer than 325 nm are observed. The coating with TiO_2 without Ag presents the highest transmittance values. As long as the silver content increases, T_{fg} decreases, being this behavior more noticeable between 350 and 400 nm. On the contrary, reflectance spectra are similar for all tested samples.

Employing Eqs. (6) and (7) and the experimental values of transmittance and reflectance presented in Fig. 3, $T_{f,\lambda}$ and $R_{f,\lambda}$ were computed, and then $\alpha_{f,\lambda}$ between 300 and 400 nm was calculated with Eq. (5).

Fig. 4 shows the fraction of energy absorbed by the different coatings ($\alpha_{f,\lambda}$). From 300 to 340 nm, all the coatings rendered values of $\alpha_{f,\lambda}$ above 0.90. For longer wavelengths, the absorbed energy decreases. At 400 nm, the lowest value corresponds to the coating with TiO_2 alone. As long as the amount of silver increases in the coating, the fraction of absorbed energy also increases.

Only the anatase phase was identified from X-ray diffraction patterns of the TiO_2 film without silver and with 1.09 wt.% Ag/TiO_2. Using the Scherrer approximation, the average grain size of the anatase phase was estimated from the intensity of anatase (1 0 1) peak ($2\theta = 25.35°$, Cu Kα). As can be deduced from results presented in Table 1, the addition of silver has no significant effect on the anatase grain size. It should be also noted that the particle size specified by the manufacturer is 20 nm. Presumably due to the small quantity of catalyst present on each sample, it was not possible to observe the rutile crystalline phase or the Ag presence with this technique.

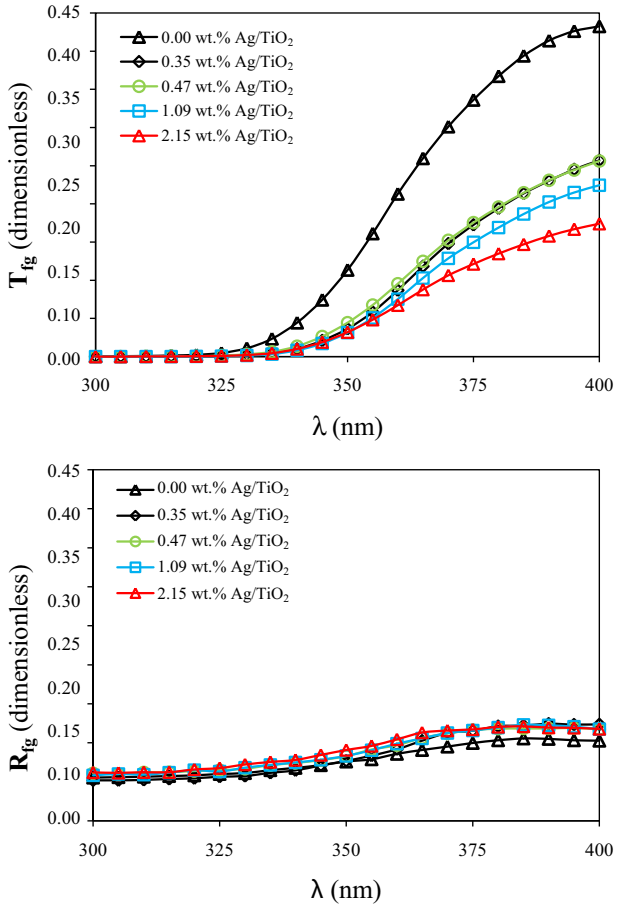

Fig. 3. Experimental transmittance (T_{fg}) and reflectance (R_{fg}) values of the coated plates.

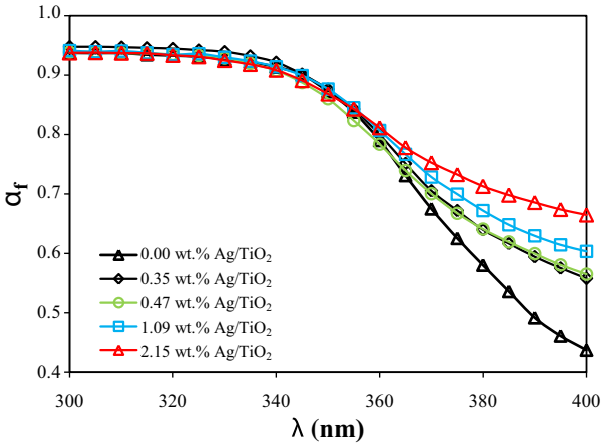

Fig. 4. Fraction of energy absorbed ($\alpha_{f,\lambda}$) by the different coatings.

AFM images of the tested films are shown in Fig. 5. The AFM method provides an evaluation of the relative surface roughness expressed as the roughness average value, summarized in Table 1, obtained from topography images, Fig. 5(a) and (c).

Because the same preparation procedure was employed for both samples, the AFM pictures reflect the influence of the Ag deposits on the surface. The TiO_2 surface has an average roughness of 32.35 nm. A slight decrease of the roughness was observed for TiO_2 with Ag (26.40 nm). This effect can be observed more clearly in phase images (Fig. 5(b) and (d)).

Ag content results obtained from XPS analysis are also given in Table 1. This content expresses the atomic ratio between Ag and Ti on the surface of the films.

3.2. Spore inactivation

Fig. 6 shows the experimental values of viable spores concentration as a function of the irradiation time for the TiO_2 and the Ag/TiO_2 coatings. The corresponding fitting curves are also depicted in the figure.

Table 2 presents the estimated values of the apparent kinetic parameter k in Eq. (7), with the corresponding 99% confidence interval, for the coatings with TiO_2 and with different amounts of Ag added. The orders of magnitude reduction of the initial concentration of viable bacteria after 6 h of irradiation are also presented in the table. There is a significant increase in the apparent kinetic constant as the Ag content increases, reaching a maximum value at 1.09 wt.% Ag/TiO_2. However, a lower value of k was obtained when the ratio Ag/TiO_2 in the coating was 2.15 wt.%.

As observed in Fig. 6 and Table 2, when the 1.09 wt.% Ag/TiO_2 coating was tested, a decrease greater than 3 orders of magnitude in the viable spore concentration was obtained after 6 h of irradiation (from 3.71×10^5 to 1.29×10^2 CFU cm^{-2}). In contrast, when the TiO_2 coating was employed, the decrease was less than 2 orders of magnitude considering the same irradiation time (from 1.84×10^5 to 3.40×10^3 CFU cm^{-2}).

No significant changes in the survival of spores were observed when samples were kept in the dark over the TiO_2 and Ag/TiO_2 films. Results of the apparent kinetic constants in dark conditions were 0.016 h^{-1} with TiO_2 alone and 0.015 h^{-1} with 1.09 wt.% Ag/TiO_2, 2 orders of magnitude smaller than the values of k obtained with the irradiated catalysts. Based on these results, the bacterici-

Table 1
Characterization of the photocatalytic films.

Ag/TiO_2 (wt.%)	TiO_2 particle size (nm)	Anatase (%)	Roughness average (nm)	Superficial Ag/Ti content (%)
0.00	19.9	36.3	32.3	0.0
1.09	20.2	32.1	26.4	11.0

dal action of silver over spores can be considered negligible when samples are not irradiated. Additionally, no significant variations in the concentration of viable spores were obtained when samples were exposed to UV radiation in the absence of photocatalysts (over bare plates). The value of k without catalyst was 0.011 h^{-1}.

Fig. 7 presents SEM images of the spores over TiO_2 and Ag/TiO_2-coatings, before and after 6 h of photocatalytic treatment. Clear morphological changes are observed in the spores after treatment, including reduction of size and irregularities in the spore surface (for comparison purposes, the size of the red oval is the same in all images). These changes suggest progressive damage of the spore structure with the treatment, especially when the Ag/TiO_2 coating is employed.

3.3. Evaluation of photocatalytic efficiencies

Values of the initial rate of inactivation and of the energy absorbed by the coated plates calculated with Eq. (4) are shown in Table 3. The initial spore concentration is known to be 3.00×10^5 CFU cm^{-2}. From this information, the quantum efficiency of inactivation for the different coatings was calculated (Eq. (9)), and results are also presented in Table 3. The highest quantum efficiency was obtained for the coating with 1.09 wt.% Ag/TiO_2.

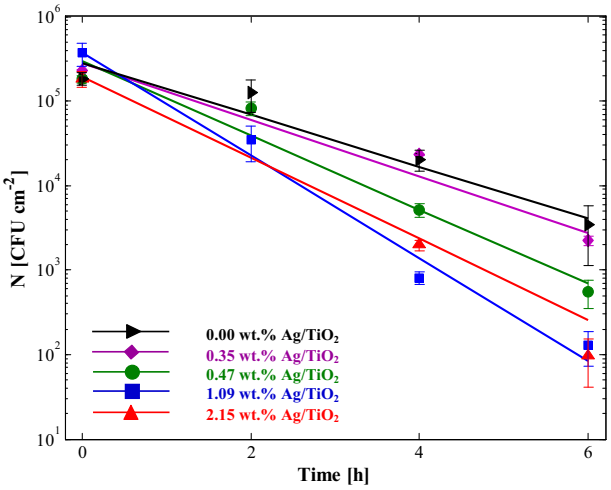

Fig. 6. Viable spore concentration vs irradiation time over TiO_2 and Ag/TiO_2 coated plates. Error bars represent 99% confidence interval.

3.4. Enhanced activity of Ag/TiO_2 coatings

Highly reactive oxygen species (ROS) are believed to be the main species responsible for the photocatalytic inactivation of microorganisms by damaging the cell wall and membrane [5,25]. Silver could enhance the antibacterial effect of photocatalysis by acting as an electron trap at the surface of TiO_2, thus reducing charge recombination and facilitating the reaction of holes with adsorbed water to form hydroxyl radicals. Additionally, direct oxidation of cell components by holes could be enhanced. Based on

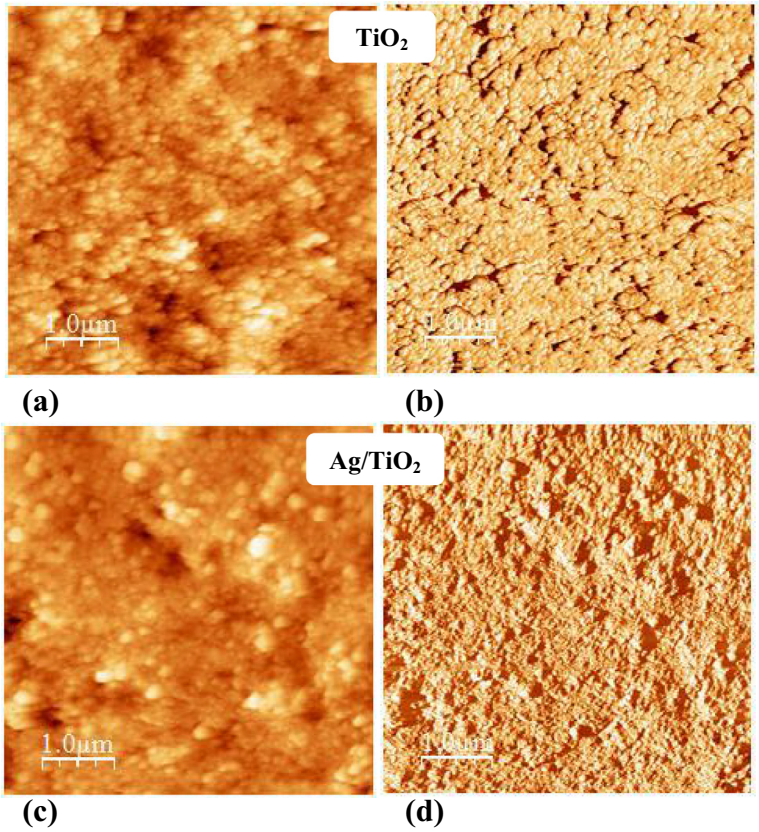

Fig. 5. AFM pictures of TiO_2 and 1.09 wt.% Ag/TiO_2 films. (a) and (c) topography images, and (b) and (d) phase images.

Table 2
Apparent kinetic parameters and orders of magnitude reduction.

Ag/TiO_2 (wt.%)	k (h^{-1})	Orders of magnitude reduction after 6 h of irradiation
0.00	0.705 ± 0.059	1.7
0.35	0.771 ± 0.059	2.0
0.47	1.011 ± 0.062	2.5
1.09	1.397 ± 0.078	3.5
2.15	1.102 ± 0.112	3.3

the information reported in Table 1, the addition of silver does not significantly modify the surface properties of the films.

A notable increase in the inactivation activity was observed by increasing the silver content of the coatings, reaching a maximum quantum efficiency with the sample containing 1.09 wt.% Ag/TiO_2 ($\eta_{abs} = 4.18 \times 10^{-14}$ CFU photon^{-1}, Table 3). Nevertheless, an important decrease of the quantum efficiency was found with 2.15 wt.% Ag/TiO_2. Evidently, there is an optimum silver content. An excess of metal could reduce the catalyst activity by (i) blocking the active sites of the catalyst, and (ii) acting as a recombination site itself [26,27]. Concerning this last effect, He et al. [28] studied the influence of Ag doping in the photocatalytic activity of TiO_2. They found an optimal Ag concentration. Within a proper range, silver inhibits electron–hole recombination and the photocatalytic activity increases with increasing silver concentration. On the other hand, when silver content exceeds an optimum value, holes in the interfacial region of TiO_2 film may be trapped by the Ag particles before they react with the surface hydroxyl ions and water, leading to a reduction in the quantum efficiency.

Silver alone exhibits deleterious effects over vegetative bacteria by different mechanisms, including direct damage of the cell membrane, and extracellular and intracellular generation of ROS [14]. Nevertheless, these bactericidal effects were not detected in our study when *B. subtilis* spores were kept in the dark over Ag/TiO_2 coatings. An explanation can be found in the distinctive characteristics of the spore structure, containing a coat, a cortex and a dehydrated core that protect the cell from adverse environmental conditions. Due to these reasons, it can be assumed that, at the beginning of the photocatalytic process, silver acts as an electron trap, accelerating the generation of ROS and thus increasing the rate of spore inactivation. As long as the reaction proceeds, the spore cortex and coat are progressively damaged, they become more vulnerable and, at that moment, the silver bactericidal activity could also take place.

4. Conclusions

The inactivation of *B. subtilis* spores spread over TiO_2 films irradiated with artificial UV-A light was clearly enhanced by Ag deposition. The performance of the Ag/TiO_2 catalyst with four different Ag amounts was compared with the activity of TiO_2 without Ag,

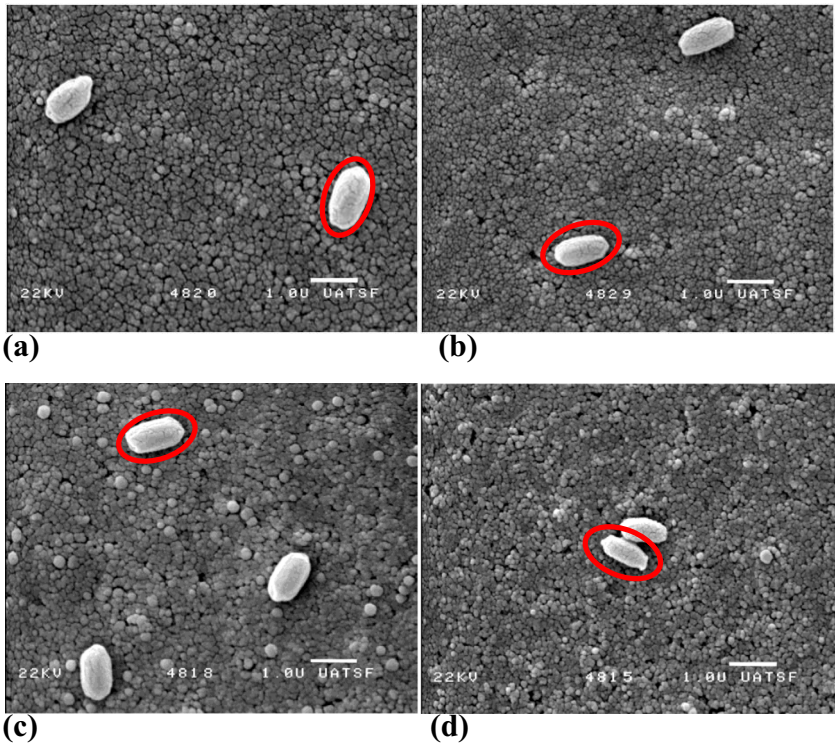

Fig. 7. SEM images. TiO_2 coating: (a) unirradiated, (b) after 6 h irradiation. Ag/TiO_2 coating: (c) unirradiated and (d) after 6 h irradiation.

Table 3
Initial rate of inactivation, absorbed energy and quantum efficiency of inactivation employing coatings with different silver contents.

Ag/TiO_2 (wt.%)	$-(dN/dt)\|_{t=0}$ [CFU cm^{-2} h^{-1}]	$\langle e^{a,s}\rangle_{A_{irr}}$ [photon cm^{-2} h^{-1}]	$\eta_{abs} \times 10^{14}$ [CFU photon^{-1}]
0.00	2.12×10^5	9.66×10^{18}	2.19
0.35	2.31×10^5	9.94×10^{18}	2.33
0.47	3.03×10^5	9.80×10^{18}	3.09
1.09	4.19×10^5	1.00×10^{19}	4.18
2.15	3.31×10^5	1.01×10^{19}	3.27

using the quantum efficiency parameter. A significant increase in the inactivation was found when the silver content of the coatings increased, reaching a maximum quantum efficiency with the sample containing 1.09 wt.% Ag/TiO_2. However, an important decrease of the quantum efficiency was observed with an excess of the deposited metal (2.15 wt.% Ag/TiO_2).

The increased antibacterial activity of the silver loaded samples can be associated to the fact that silver acts as electron trap at the TiO_2 surface. Accordingly, the reduction of charge recombination facilitates the generation of reactive oxygen species and the inactivation of bacterial spores. Nevertheless, the optimum silver amount must be determined because an excess of metal could be detrimental for the photocatalytic process.

It can be concluded that the use of silver significantly reduces the inactivation treatment time, making this technology more attractive for practical applications. Additionally, the value of the quantum efficiency of inactivation shows how efficiently the absorbed radiation is employed to inactivate microorganisms, giving an indirect insight into the photocatalytic mechanism. More knowledge related to photon absorption and electron transfer mechanisms is needed to be able of enhancing or inhibiting particular events in photocatalytic surfaces.

Acknowledgements

The authors are grateful to Universidad Nacional del Litoral (UNL), Consejo Nacional de Investigaciones Científicas y Técnicas (CONICET), and Agencia Nacional de Promoción Científica y Tecnológica (ANPCyT) for the financial support. They also thank Antonio C. Negro for his help during the experimental work, Dr. Mario Passeggi for his technical assistance with the AFM measurements, and Professor María C. Lurá for her valuable support. Thanks are given to ANPCyT for the purchase of the SPECS multitechnique analysis instrument (PME8-2003).

References

[1] Z.D. Bolashikov, A.K. Melikov, Methods for air cleaning and protection of building occupants from airborne pathogens, Build. Environ. 44 (2009) 1378–1385.
[2] C.Y. Lin, C.S. Li, Inactivation of microorganisms on the photocatalytic surfaces in air, Aerosol Sci. Technol. 37 (2003) 939–946.
[3] B.U. Lee, Life comes from the air: a short review on bioaerosol control, Aerosol Air Qual. Res. 11 (2011) 921–927.
[4] F. Chen, X. Yang, H.K.C. Mak, D.W.T. Chan, Photocatalytic oxidation for antimicrobial control in built environment: a brief literature overview, Build. Environ. 45 (2010) 1747–1754.
[5] H.A. Foster, I.B. Ditta, S. Varghese, A. Steele, Photocatalytic disinfection using titanium dioxide: spectrum and mechanism of antimicrobial activity, Appl. Microbiol. Biotechnol. 90 (2011) 1847–1868.
[6] A. Markowska-Szczupak, K. Ulfig, A.W. Morawski, The application of titanium dioxide for deactivation of bioparticulates: an overview, Catal. Today 169 (2011) 249–257.
[7] J. Zhao, V. Krishna, B. Hua, B. Moudgil, B. Koopman, Effect of UV-A irradiance on photocatalytic and UV-A inactivation of *Bacillus cereus* spores, J. Photochem. Photobiol. B94 (2009) 96–100.
[8] N.T.T. Le, H. Nagata, M. Aihara, A. Takahashi, T. Okamoto, T. Shimohata, K. Mawatari, Y. Kinouchi, M. Akutagawa, M. Haraguchi, Additional effects of silver nanoparticles on bactericidal efficiency depend on calcination temperature and dip-coating speed, Appl. Environ. Microbiol. 77 (2011) 5629–5634.
[9] A. Vohra, D.Y. Goswami, D.A. Deshpande, S.S. Block, Enhanced photocatalytic inactivation of bacterial spores on surfaces in air, J. Ind. Microbiol. Biotechnol. 32 (2005) 364–370.
[10] E.A. Kozlova, A.S. Safatov, S.A. Kiselev, V.YU. Marchenko, A.A. Sergeev, M.O. Skarnovich, E.K. Emelyanova, M.A. Smetannikova, G.A. Buryak, A.V. Vorontsov, Inactivation and mineralization of aerosol deposited model pathogenic microorganisms over TiO_2 and Pt/TiO_2, Environ. Sci. Technol. 44 (2010) 5121–5126.
[11] M. Sökmen, F. Candan, Z. Sumer, Disinfection of *E. coli* by the Ag–TiO_2/UV system: lipidperoxidation, J. Photochem. Photobiol., A 143 (2001) 241–244.
[12] R. van Grieken, J. Marugán, C. Sordo, P. Martínez, C. Pablos, Photocatalytic inactivation of bacteria in water using suspended and immobilized silver–TiO_2, Appl. Catal. B 93 (2009) 112–118.
[13] S. Malato, P. Fernández-Ibáñez, M.I. Maldonado, J. Blanco, W. Gernjak, Decontamination and disinfection of water by solar photocatalysis: recent overview and trends, Catal. Today 147 (2009) 1–59.
[14] C. Marambio-Jones, E.M.V. Hoek, A review of the antibacterial effects of silver nanomaterials and potential implications for human health and the environment, J. Nanopart. Res. 12 (2010) 1531–1551.
[15] M. Montazer, A. Behzadnia, E. Pakdel, M.K. Rahimi, M.B. Moghadam, Photo induced silver on nano titanium dioxide as an enhanced antimicrobial agent for wool, J. Photochem. Photobiol., A 103 (2011) 207–214.
[16] C.A. Castro, P. Osorio, A. Sienkiewicz, C. Pulgarin, A. Centeno, S.A. Giraldo, Photocatalytic production of $^1O_2$ and ·OH mediated by silver oxidation during the photoinactivation of *Escherichia coli* with TiO_2, J. Hazard. Mater. 211–112 (2012) 172–181.
[17] H. De Lasa, B. Serrano, M. Salaices, Photocatalytic Reaction Engineering, Springer, New York, 2005.
[18] S.M. Zacarías, M.L. Satuf, M.C. Vaccari, O.M. Alfano, Efficiency evaluation of different TiO_2 coatings on the photocatalytic inactivation of airborne bacterial spores, Ind. Eng. Chem. Res. 51 (2012) 13599–13608.
[19] T.E. Shehata, E.B. Collins, Sporulation and heat resistance of psychrophilic strains of *Bacillus*, J. Dairy Sci. 55 (1972) 1405–1409.
[20] S.M. Zacarías, M.C. Vaccari, H.A. Irazoqui, G.E. Imoberdorf, O.M. Alfano, Effect of the radiation flux on the photocatalytic inactivation of spores of *Bacillus subtilis*, J. Photochem. Photobiol., A 214 (2010) 171–180.
[21] R. van Grieken, J. Marugán, C. Sordo, C. Pablos, Comparison of the photocatalytic disinfection of *E. coli* suspensions in slurry, wall and fixed-bed reactors, Catal. Today 144 (2009) 48–54.
[22] N.B. Jackson, C.M. Wang, Z. Luo, J. Schwitzgebel, J.G. Ekerdt, J.R. Brock, A. Heller, Attachment of TiO_2 powders to hollow glass microbeads: activity of the TiO_2-coated beads in the photoassisted oxidation of ethanol to acetaldehyde, J. Electrochem. Soc. 138 (1991) 3660–3664.
[23] R. Siegel, J. Howell, Thermal Radiation Heat Transfer, fourth ed., Taylor and Francis, New York, USA, 2002.
[24] I. Horcas, R. Fernandez, J.M. Gomez-Rodriguez, J. Colchero, J. Gomez-Herrero, A.M. Baro, WSXM: a software for scanning probe microscopy and a tool for nanotechnology, Rev. Sci. Instrum. 78 (2007) 1–8.
[25] O.K. Dalrymple, E. Stefanakos, M.A. Trotz, D.Y. Goswami, A review of the mechanisms and modeling of photocatalytic disinfection, Appl. Catal. B98 (2010) 27–38.
[26] H. Tran, K. Chiang, J. Scott, R. Amal, Clarifying the role of silver deposits on titania for the photocatalytic mineralization of organic compounds, J. Photochem. Photobiol., A 183 (2006) 41–52.
[27] A.A. Ashkarran, S.M. Aghigh, M. Kavianipour, N.J. Farahani, Visible light photo- and bioactivity of Ag/TiO_2 nanocomposite with various silver contents, Curr. Appl. Phys. 11 (2011) 1048–1055.
[28] C. He, Y. Yu, X. Hu, A. Larbot, Influence of silver doping on the photocatalytic activity of titania films, Appl. Surf. Sci. 200 (2002) 239–247.